

FINITE ELEMENT TECHNIQUES FOR THE NUMERICAL SIMULATION OF TWO-PHASE INCOMPRESSIBLE FLOWS

ARNOLD REUSKEN

- Institut für Geometrie und Praktische Mathematik, RWTH-Aachen University,
D-52056 Aachen, Germany
-

Abstract. In this paper we present an overview of finite element methods that have recently been developed for the numerical simulation of two-phase incompressible flow problems. We only consider the fluid dynamics, modeled by the Navier-Stokes equations with a surface tension force at the interface. We discuss a finite element discretization of the level set equation, the discretization of surface tension both for the case of a clean and a viscous interface, and an extended finite element method for approximation of the discontinuous pressure variable.

Keywords. finite element method, level set method, surface tension, surface viscosity, xfem

INTRODUCTION

Nowadays finite element methods form an approved technology for the discretization of *one*-phase incompressible flow problems. Concerning the application of finite element discretization methods in *two*-phase flows much less is known. In the past decade there has been a strong increase in the research on extensions of finite element techniques to the field of two-phase incompressible flow problems. In this paper we present an overview of some finite element methods that are specifically designed for the discretization of two-phase flow problems.

We restrict ourselves to the *fluid dynamics*, which is modeled by the Navier-Stokes equation with a surface tension force at the interface. For discretization we use an Eulerian approach in which the (moving) interface is captured by the level set method. Related to this we treat (in Section 2) the following four finite element topics. Firstly, a finite element discretization of the hyperbolic level set equation, which has to be stable and accurate, in particular with respect to volume conservation, is addressed. Secondly, we explain a discretization method for the surface tension force in which (discrete) second derivatives (related to interface curvature) are avoided. As a third topic we treat a finite element method for handling surface viscosity, described by the Boussinesq-Scriven model. Finally we explain how the extended finite element method (XFEM) can be used for an accurate approximation of the pressure variable, which is discontinuous across the interface.

We mention that recently special finite element techniques have also been developed for the numerical simulation of *mass transport* in two-phase flows, which is modeled by a convection-diffusion equation with a Henry condition at the interface. The XFEM technique can be combined with a method due to Nitsche, resulting in a flexible and accurate method for numerically treating the Henry condition ([16]). For the simulation of *transport of surfactants* on the interface an Eulerian finite element method can be used for the discretization of the convection-diffusion equation *on* the moving interface.

Most of these finite element methods have recently been treated in the literature. The aim of this paper is to present a compact unified overview of some methods used for the fluid dynamics problem. Therefore we only present the main ideas of these methods, while referring to the corresponding literature for more details, e.g. on theoretical (error) analyses.

FINITE ELEMENT METHODS FOR THE FLUID DYNAMICS MODEL

Mathematical model

Let $\Omega \subset \mathbb{R}^d$, $d=2,3$, be a domain containing two different immiscible incompressible phases. The time dependent subdomains containing the two phases are denoted by $\Omega_1(t)$ and $\Omega_2(t)$ with $\bar{\Omega} = \bar{\Omega}_1 \cup \bar{\Omega}_2$ and $\Omega_1 \cap \Omega_2 = \emptyset$. We assume that Ω_1 and Ω_2 are connected and $\partial\Omega_1 \cap \partial\Omega = \emptyset$ (i. e., Ω_1 is completely contained in Ω). The interface is denoted by $\Gamma(t) = \bar{\Omega}_1(t) \cap \bar{\Omega}_2(t)$. The standard model for describing incompressible two-

phase flows consists of the Navier-Stokes equations in the subdomains with the coupling condition

$$[\boldsymbol{\sigma}\mathbf{n}]_{\Gamma} = -\tau\kappa\mathbf{n}$$

at the interface, i. e., the surface tension balances the jump of the normal stress on the interface. We use the notation $[v]_{\Gamma}$ for the jump across Γ , $\mathbf{n} = \mathbf{n}_{\Gamma}$ is the unit normal at the interface Γ (pointing from Ω_1 into Ω_2), κ the curvature of Γ , τ the surface tension coefficient (assumed to be constant) and $\boldsymbol{\sigma}$ the stress tensor defined by

$$\boldsymbol{\sigma} = -p\mathbf{I} + \mu\mathbf{D}(\mathbf{u}), \quad \mathbf{D}(\mathbf{u}) = \nabla\mathbf{u} + (\nabla\mathbf{u})^T,$$

with $p = p(x, t)$ the pressure, $\mathbf{u} = \mathbf{u}(x, t)$ the velocity and μ the viscosity. We assume continuity of \mathbf{u} across the interface. Combined with the conservation laws for mass and momentum we obtain the following standard model, cf. for example [24, 31, 30, 16],

$$\begin{cases} \rho_i \frac{\partial \mathbf{u}}{\partial t} - \operatorname{div}(\mu_i \mathbf{D}(\mathbf{u})) + \rho_i (\mathbf{u} \cdot \nabla) \mathbf{u} + \nabla p = \rho_i \mathbf{g} & \text{in } \Omega_i \times [0, T], i = 1, 2, \\ \operatorname{div} \mathbf{u} = 0 & \text{in } \Omega_i \times [0, T] \end{cases} \quad (1)$$

$$[\boldsymbol{\sigma}\mathbf{n}]_{\Gamma} = -\tau\kappa\mathbf{n}, \quad [\mathbf{u}]_{\Gamma} = 0. \quad (2)$$

The constants μ_i, ρ_i denote viscosity and density in the subdomain Ω_i , $i = 1, 2$, and \mathbf{g} is an external volume force (gravity). To make this problem well-posed we need suitable boundary conditions for \mathbf{u} and an initial condition for \mathbf{u} . For simplicity we restrict to homogeneous Dirichlet boundary conditions for \mathbf{u} .

The location of the interface $\Gamma(t)$ is in general unknown and is coupled to the local flow field which transports the interface. For immiscible fluids this transport of the interface is modeled by $V_{\Gamma} = \mathbf{u} \cdot \mathbf{n}$, where V_{Γ} denotes the normal velocity of the interface.

One very popular method for numerically capturing the moving interface $\Gamma(t)$ is based on the level set method [28, 27, 23]. We briefly recall the main idea. The inflow part of the boundary is given by $\partial\Omega^- := \{x \in \partial\Omega \mid \mathbf{u}(x) \cdot \mathbf{n}_{\Omega}(x) < 0\}$. For given sufficiently smooth boundary data g and initial condition ϕ_0 we consider the problem of finding a solution $\phi = \phi(x, t)$, $x \in \Omega, t \in [0, T]$, of the level set equation

$$\begin{aligned} \frac{\partial \phi}{\partial t} + \mathbf{u} \cdot \nabla \phi &= 0 & \text{in } \Omega \\ \phi &= g & \text{on } \partial\Omega^- \\ \phi(\cdot, 0) &= \phi_0 & \text{in } \Omega. \end{aligned} \quad (3)$$

The velocity field \mathbf{u} used in (3) results from the Navier-Stokes equations. The boundary data g may depend on t , and the initial condition ϕ_0 is assumed to satisfy $\phi_0(x) = g(x,0)$ for $x \in \partial\Omega^-$. The initial condition is chosen such that $\{x | \phi_0(x) = 0\} = \Gamma(0)$ and ϕ_0 is (approximately) a signed distance function to $\Gamma(0)$. From the definition of the transport equation in (3) it follows that $\Gamma(t) = \{x | \phi(x,t) = 0\}$, i.e., the interface is given by the zero level of $\phi(x,t)$.

Discretization of the level set equation

If a conforming finite element discretization is applied to the linear hyperbolic level set equation, a suitable stabilization is necessary. One very popular technique is the standard SUPG method (also often called streamline diffusion finite element method). Alternatively one could use a discontinuous Galerkin approach (DG), cf. [2, 17]. Here we only consider the SUPG method. Let $\{\mathbb{T}_h\}_{h>0}$ be a family of shape regular tetrahedral triangulations of Ω . For simplicity we restrict to triangulations \mathbb{T}_h that are quasi-uniform. The parameter h denotes the maximal diameter: $h = \max_{T \in \mathbb{T}_h} h_T$, with $h_T = \text{diam}(T)$. Let V_h^k be the standard polynomial finite element space:

$$V_h^k = \{v_h \in C(\Omega) | (v_h)|_T \in \mathbf{P}_k \text{ for all } T \in \mathbb{T}_h\}, \quad k \geq 1.$$

For the level set equation one typically has an inhomogeneous boundary condition on the inflow boundary. This can be treated in different ways, for example, as a weakly imposed condition incorporated in the bilinear form (as in [19]) or as an essential condition in the finite element space. We use the latter approach since it fits better to the analysis in [7]. For this we introduce the set of points on the inflow boundary $\partial\Omega^-$ that correspond to degrees of freedom in the finite element space V_h^k . This set is denoted by $V(\partial\Omega^-)$. For a given $f \in C(\partial\Omega^-)$ we define

$$V_h^k(f) = \{v_h \in V_h^k | v_h(x) = f(x) \text{ for all } x \in V(\partial\Omega^-)\}.$$

The L^2 -scalar product on Ω and corresponding norm are denoted by (\cdot, \cdot) and $\|\cdot\|$, respectively. The SUPG semi-discretization of the level set equation (3) is as follows: For $t \in [0, T]$ determine $\phi_h(\cdot, t) \in V_h^k(g(t))$ with $\phi_h(\cdot, 0) = \phi_{0,h}$ such that

$$\left(\frac{\partial \phi_h}{\partial t} + \mathbf{u} \cdot \nabla \phi_h, v_h + \delta \mathbf{u} \cdot \nabla v_h\right) = 0 \quad \text{for all } v_h \in V_h^k(0). \quad (4)$$

For the stabilization parameter δ we take the value $\delta = \frac{h}{\|\mathbf{u}\|_{L^\infty(\Omega)}}$. The discrete initial

condition $\phi_{0,h} \in V_h^k(\phi_0)$ is a (sufficiently accurate) finite element approximation of ϕ_0 . The space discretization (4) can be combined with finite difference approximations of the time derivative. In [7] the implicit Euler, Crank-Nicolson (CN) and BDF2 time discretizations are analyzed in a general setting. To simplify the presentation, we restrict to the CN method. Combination of the SUPG spatial discretization with the CN time discretization results in a fully discrete problem with a sequence of finite element functions $\phi_h^n \in V_h^k(g(t_n))$, $1 \leq n \leq N$, with $N\Delta t = T$, $t_n := n\Delta t$. The initialization is given by $\phi_h^0 = \phi_{0,h}$, and for $n \geq 1$ the discrete solution $\phi_h^n \in V_h^k(g(t_n))$ is defined by

$$\left(\frac{\phi_h^n - \phi_h^{n-1}}{\Delta t} + \frac{1}{2}\mathbf{u} \cdot \nabla(\phi_h^n + \phi_h^{n-1}), v_h + \delta \mathbf{u} \cdot \nabla v_h\right) = 0 \quad \text{for all } v_h \in V_h^k(0). \quad (5)$$

For this method a discretization error analysis was recently given in [7]. In this analysis is assumed that the level set function ϕ has sufficient regularity such that higher derivatives of ϕ , that occur in the error bounds, exist (at least close to the interface). For the SUPG-CN approximation $\phi_h^N \in V_h^k(g(T))$ of $\phi(\cdot, T)$ the error bound

$$\|\phi_h^N - \phi(\cdot, T)\| + \delta \|\mathbf{u} \cdot \nabla(\phi_h^N - \phi(\cdot, T))\| \leq cT(h^{k+\frac{1}{2}} + \Delta t^2) \quad (6)$$

is proved. The constant c depends on the smoothness of the data g and the solution ϕ , but does not depend on T , h , Δt . In view of surface tension approximation (cf. Section 2.3) the case $k=2$, i.e. quadratic finite elements, is particularly relevant. The error analysis shows that the SUPG is a stable method that results in accurate approximations (at least second order accurate for $k=2$). Furthermore, due to the control on the derivative of the error in streamline direction there are only (very) weak numerical oscillations. Results of numerical experiments which quantify these observations are given in e.g. [7, 25]. In the context of incompressible flows the issue of volume conservation is important. Due to incompressibility

one has $\frac{d}{dt}V(t) = 0$, where $V(t) = \text{int}(\Gamma(t))$ denotes the volume (in 3D) of the phase

contained in the interior of $\Gamma(t)$. The discrete interface at time T is given by

$\Gamma_h = \{x | \phi_h^N(x) = 0\}$, with ϕ_h^N the discrete level set solution defined in (5). In [25] it is shown

that, under reasonable assumptions e.g. on the choice of Δt and on the smoothness of Γ_h , the

discrete interface $\Gamma_h = \Gamma_h(T)$ is close to $\Gamma = \Gamma(T)$ in the following sense. The error bounds

$$\|d\|_{L^2(\Gamma_h)} \leq ch^k, \quad |V - V_h| \leq ch^k,$$

hold, with $d(x)$ the signed distance function to Γ , $V = V(T)$ and $V_h = \text{int}(\Gamma_h)$ the volume of the phase contained in the interior of Γ_h . These results show that although there is no exact volume conservation the error is of acceptable size (second order for $k=2$) and can be controlled, e.g. by the order k of the finite elements used. We refer to [25] for results of numerical experiments that illustrate the predicted good performance w.r.t. volume conservation. We emphasize that for the results outlined above it is essential that, close to the interface $\Gamma(t)$, the level set function ϕ behaves smoothly (more precise: is close to a signed distance function). In practice this is realized by using a suitable re-initialization procedure. We do not treat this topic here.

Discretization of the surface tension force

We assume the surface tension coefficient τ in (2) to be constant. For capturing the interface we use a level set method with SUPG discretization as outlined above, and $k=2$. The condition $k \geq 2$ is, at least in the approach presented below, essential for getting satisfactory approximations of the surface tension force (which involves the curvature of the interface). A discrete interface approximation can be constructed as follows. The piecewise quadratic finite element approximation of ϕ on a tetrahedral triangulation (in 3D) \mathbb{T}_h is denoted by ϕ_h . Note that in general it is not easy to determine the zero level of ϕ_h . Therefore an additional approximation is introduced. We use one further refinement of \mathbb{T}_h , denoted by \mathbb{T}'_h , that is obtained by regular subdivision of each tetrahedron into 8 child tetrahedra. Let $I(\phi_h)$ be the continuous piecewise *linear* function on \mathbb{T}'_h which interpolates ϕ_h at all vertices of all tetrahedra in \mathbb{T}'_h . The approximation of the interface Γ is defined by

$$\Gamma_h := \{x \in \Omega \mid I(\phi_h)(x) = 0\} \quad (7)$$

and consists of piecewise planar segments that are easy to compute.

In the *weak* formulation of the fluid dynamics problem the surface tension interface condition $[\boldsymbol{\sigma}\mathbf{n}]_\Gamma = -\tau\boldsymbol{\kappa}\mathbf{n}$ is represented by a linear *functional*

$$f_\Gamma(\mathbf{v}) := -\tau \int_\Gamma \boldsymbol{\kappa}\mathbf{v} \cdot \mathbf{n} ds \quad (8)$$

with \mathbf{v} a velocity test vector function and \mathbf{n} the unit normal on Γ . In a Galerkin finite element discretization we only use $\mathbf{v} = \mathbf{v}_h$ from a finite element space (e.g. piecewise

quadratics). In many numerical simulations of two-phase flows, the discretization of the curvature κ is a very delicate issue. This is related to the fact that κ contains *second* derivatives. One way to express these second derivatives is by means of the Laplace-Beltrami characterization of the mean curvature:

$$-\Delta_\Gamma \text{id}_\Gamma(x) = \kappa(x)\mathbf{n}(x), \quad x \in \Gamma. \quad (9)$$

In the variational formulation we have the possibility to lower the order of differentiation by shifting one of the derivatives to the test function. Using this, we see that (8), with $\mathbf{v} = \mathbf{v}_h$, can be rewritten as follows:

$$f_\Gamma(\mathbf{v}_h) = -\tau \int_\Gamma \nabla_\Gamma \text{id}_\Gamma \cdot \nabla_\Gamma \mathbf{v}_h \, ds, \quad \mathbf{v}_h \in \mathbf{V}_h, \quad (10)$$

where \mathbf{V}_h denotes the velocity finite element space. In this variational setting it is natural to use the expression on the right-hand side in (10) as a starting point for the discretization of the surface tension force. This idea is used in, for example, [8, 3, 12, 13, 18, 22]. In this discretization we use the approximation Γ_h of Γ . Given this approximate interface Γ_h , the localized force term $f_\Gamma(\mathbf{v}_h)$ is approximated by

$$f_{\Gamma_h}(\mathbf{v}_h) := -\tau \int_{\Gamma_h} \nabla_{\Gamma_h} \text{id}_{\Gamma_h} \cdot \nabla_{\Gamma_h} \mathbf{v}_h \, ds, \quad \mathbf{v}_h \in \mathbf{V}_h. \quad (11)$$

In [15] an error analysis for this discretization is given. Based on that analysis, it is natural to introduce the following modified, more accurate, variant of the functional f_{Γ_h} . Define the orthogonal projection

$$\mathbf{P}_h(x) := \mathbf{I} - \mathbf{n}_h(x)\mathbf{n}_h(x)^T \quad \text{for } x \in \Gamma_h, x \text{ not on an edge,}$$

where \mathbf{n}_h is the unit normal on Γ_h (pointing outward from Ω_1). The tangential derivative along Γ_h can be written as $\nabla_{\Gamma_h} g = \mathbf{P}_h \nabla g$. Note that

$$\nabla_{\Gamma_h} \text{id}_{\Gamma_h} = \mathbf{P}_h \nabla \text{id}_{\Gamma_h} = (\mathbf{P}_h e_1, \mathbf{P}_h e_2, \mathbf{P}_h e_3)^T,$$

with e_i the i -th standard basis vector in \mathbf{R}^3 . Thus the functional f_{Γ_h} can be written as

$$\begin{aligned} f_{\Gamma_h}(\mathbf{v}_h) &= -\tau \int_{\Gamma_h} \mathbf{P}_h \nabla \text{id}_{\Gamma_h} \cdot \nabla_{\Gamma_h} \mathbf{v}_h \, ds \\ &= -\tau \sum_{i=1}^3 \int_{\Gamma_h} \mathbf{P}_h e_i \cdot \nabla_{\Gamma_h} v_i \, ds, \quad v_i := (\mathbf{v}_h)_i. \end{aligned} \quad (12)$$

The discrete interface Γ_h is constructed as the zero level of $I\phi_h$, where ϕ_h is a piecewise *quadratic* function. This piecewise quadratic function contains better information about the

curvature of Γ than its piecewise linear interpolation $I\phi_h$ that is used for the construction of Γ_h . An improved projection $\tilde{\mathbf{P}}_h$ based on ϕ_h can be defined as follows:

$$\tilde{\mathbf{n}}_h(x) := \frac{\nabla \phi_h(x)}{\|\nabla \phi_h(x)\|}, \quad \tilde{\mathbf{P}}_h(x) := \mathbf{I} - \tilde{\mathbf{n}}_h(x)\tilde{\mathbf{n}}_h(x)^T, \quad x \in \Gamma_h. \quad (13)$$

Hence an obvious modification is given by

$$\begin{aligned} \tilde{f}_{\Gamma_h}(\mathbf{v}_h) &= -\tau \int_{\Gamma_h} \tilde{\mathbf{P}}_h \nabla \text{id}_{\Gamma_h} \cdot \nabla_{\Gamma_h} \mathbf{v}_h \, ds \\ &= -\tau \sum_{i=1}^3 \int_{\Gamma_h} \tilde{\mathbf{P}}_h e_i \cdot \nabla_{\Gamma_h} v_i \, ds, \quad v_i := (\mathbf{v}_h)_i. \end{aligned} \quad (14)$$

In [15] an error analysis is presented which shows that this discretization of the surface tension force is (significantly) better than the one in (11).

Treatment of interface viscosity with the Boussinesq-Scriven model

In modeling the rheological properties of *particle-laden interfaces* one often introduces an *effective surface viscosity* [20, 21]. A standard mathematical description of this is by means of the so-called *Boussinesq-Scriven model* which we now introduce, cf. also [29, 6, 26]. First we recall that for the bulk fluid, based on the Cauchy stress principle and assuming the Newtonian stress tensor form $\boldsymbol{\sigma} = -p\mathbf{I} + L(\mathbf{D}(\mathbf{u}))$, with a linear operator L , one can derive the Newtonian stress tensor representation

$$\boldsymbol{\sigma} = -p\mathbf{I} + \lambda \operatorname{div} \mathbf{u}\mathbf{I} + \mu \mathbf{D}(\mathbf{u}). \quad (15)$$

The Boussinesq-Scriven model starts from the (rheological) assumption that the interface behaves like a two-dimensional Newtonian fluid. In analogy with the approach for a Newtonian fluid in the bulk phase, we start from the structural assumption that on each (small) connected surface segment $\gamma \subset \Gamma$ there is a contact force on $\partial\gamma$ of the form

$$\boldsymbol{\sigma}_\Gamma n, \quad \text{with } \boldsymbol{\sigma}_\Gamma = \boldsymbol{\alpha}\mathbf{P} + L(\mathbf{D}_\Gamma(\mathbf{u})), \quad \mathbf{D}_\Gamma(\mathbf{u}) := \mathbf{P}(\nabla_\Gamma \mathbf{u} + (\nabla_\Gamma \mathbf{u})^T)\mathbf{P},$$

with L a linear operator. The unit vector n is normal to $\partial\gamma$ and tangential to Γ . Recall that $\mathbf{P} = \mathbf{I} - \mathbf{m}\mathbf{m}^T$ is the orthogonal projection onto Γ . This projection is used, since $\boldsymbol{\sigma}_\Gamma n = \boldsymbol{\sigma}_\Gamma \mathbf{P}n$ should represent only contact forces that are tangential to the surface. Note that for $L=0$ this contact force reduces to the surface tension contact force $\boldsymbol{\sigma}_\Gamma n = \boldsymbol{\alpha}\mathbf{P}n = \boldsymbol{\alpha}n$. Using the same principles (isotropy, independence of the frame of reference) as in the derivation of (15) it can be shown, cf. [29, 1], that the interface stress tensor $\boldsymbol{\sigma}_\Gamma$ must have the following form:

$$\boldsymbol{\sigma}_\Gamma = \boldsymbol{\alpha}\mathbf{P} + \tilde{\lambda}_\Gamma \operatorname{div}_\Gamma \mathbf{u}\mathbf{P} + \mu_\Gamma \mathbf{D}_\Gamma(\mathbf{u}), \quad (16)$$

with parameters $\tilde{\lambda}_\Gamma$, μ_Γ . This is the interface analogon of the bulk stress tensor representation in (15). Note that in general $\operatorname{div}_\Gamma \mathbf{u} \neq 0$, even if $\operatorname{div} \mathbf{u} = 0$ holds. In case of viscous behavior of the interface one takes $\mu_\Gamma > 0$. In a finite element setting the implementation of this surface viscosity is essentially the same as that of the surface tension force for a clean interface as described in Section 2.3. We outline the main idea. In the viscous interface case we have an interface force balance condition of the form

$$[\boldsymbol{\sigma}_\Gamma] = \operatorname{div}_\Gamma(\boldsymbol{\sigma}_\Gamma), \quad (17)$$

with an interface stress tensor $\boldsymbol{\sigma}_\Gamma$ as in (16). In the weak formulation, instead of the surface tension functional $f_\Gamma(\mathbf{v}) = -\tau \int_\Gamma \boldsymbol{\kappa} \cdot \mathbf{v} ds$ as in (8) we have the generalization

$$f_\Gamma(\mathbf{v}) = \int_\Gamma \operatorname{div}_\Gamma(\boldsymbol{\sigma}_\Gamma) \cdot \mathbf{v} ds.$$

We can rewrite this using partial integration, resulting in the viscous surface tension functional

$$f_\Gamma(\mathbf{v}) = -\sum_{i=1}^3 \int_\Gamma (e_i^T \boldsymbol{\sigma}_\Gamma) \nabla_\Gamma v_i ds, \quad (18)$$

with $\mathbf{v} = (v_1, v_2, v_3)^T$. The numerical discretization of this force can be realized very similar to that in (14):

$$\tilde{f}_\Gamma(\mathbf{v}_h) = -\sum_{i=1}^3 \int_{\Gamma_h} (e_i^T \boldsymbol{\sigma}_\Gamma^h) \nabla_{\Gamma_h} v_i ds,$$

with $v_i = (\mathbf{v}_h)_i$ and

$$\boldsymbol{\sigma}_\Gamma^h = \tilde{\boldsymbol{\pi}}_h + \tilde{\lambda}_\Gamma (\operatorname{div}_{\Gamma_h} \mathbf{u}) \tilde{\mathbf{P}}_h + \mu_\Gamma \tilde{\mathbf{P}}_h (\nabla_{\Gamma_h} \mathbf{u} + (\nabla_{\Gamma_h} \mathbf{u})^T) \tilde{\mathbf{P}}_h.$$

In the implementation of this discrete force functional one needs the same projection operator $\tilde{\mathbf{P}}_h$ as in (14) and one has to compute integrals over the approximate interface Γ_h which consists of piecewise planar segments.

XFEM for approximation of the pressure variable

We outline the basic idea of the extended finite element method (XFEM). In the setting of two-phase flow problem this method is very suitable for the approximation of the pressure, which, due to the surface tension force, is discontinuous across the interface.

Let \mathbb{T}_h be a triangulation of the domain Ω consisting of tetrahedra and let

$$V_h = \{q \in C(\Omega) \mid q|_T \in \mathbf{P}_1 \text{ for all } T \in \mathbb{T}_h\}$$

be the standard finite element space of continuous piecewise linear functions. We define the index set $\mathbf{J} = \{1, \dots, n\}$, where $n = \dim V_h$ is the number of degrees of freedom. Let $\mathbf{B} := \{q_j\}_{j=1}^n$ be the nodal basis of V_h , i. e. $q_j(x_i) = \delta_{i,j}$ for $i, j \in \mathbf{J}$ where $x_i \in \mathbf{R}^3$ denotes the spatial coordinate vector of the i -th degree of freedom.

The idea of the XFEM method is to enrich the original finite element space V_h by additional basis functions q_j^X for $j \in \mathbf{J}'$ where $\mathbf{J}' \subset \mathbf{J}$ is a given index set. An additional basis function q_j^X is constructed by multiplying the original nodal basis function q_j by a so called enrichment function Φ_j :

$$q_j^X(x) := q_j(x)\Phi_j(x). \quad (19)$$

This enrichment yields the *extended finite element space*

$$V_h^X := \text{span}(\{q_j\}_{j \in \mathbf{J}} \cup \{q_j^X\}_{j \in \mathbf{J}'}).$$

This idea was introduced in [10] and further developed in [4] for different kinds of discontinuities (kinks, jumps), which may also intersect or branch. The choice of the enrichment function depends on the type of discontinuity. For representing jumps the Heaviside function is proposed to construct appropriate enrichment functions. Basis functions with kinks can be obtained by using the distance function as enrichment function.

In our case the finite element space V_h is enriched by discontinuous basis functions q_j^X for $j \in \mathbf{J}' = \mathbf{J}_\Gamma := \{j \in \mathbf{J} \mid \text{meas}_2(\Gamma \cap \text{supp } q_j) > 0\}$, as discontinuities in the pressure only occur at the interface. Let $d : \Omega \rightarrow \mathbf{R}$ be the signed distance function (or an approximation to it) with d negative in Ω_1 and positive in Ω_2 . In our applications the discretization of the level set function φ is used for d . Then by means of the Heaviside function H we define

$$H_\Gamma(x) := H(d(x)) = \begin{cases} 0 & x \in \Omega_1 \cup \Gamma, \\ 1 & x \in \Omega_2. \end{cases}$$

As we are interested in functions with a jump across the interface we define the enrichment function

$$\Phi_j^H(x) := H_\Gamma(x) - H_\Gamma(x_j) \quad (20)$$

and a corresponding function $q_j^X := q_j \cdot \Phi_j^H$, $j \in \mathbf{J}'$. The second term in the definition of Φ_j^H is constant and may be omitted (as it does not introduce new functions in the function space), but ensures the nice property $q_j^X(x_i) = 0$, i.e. q_j^X vanishes in all degrees of freedom. As a consequence, we have

$$\text{supp } q_j^X \subset (\text{supp } q_j \cap \bigcup_{T \in \mathbb{T}_h^\Gamma} T), \quad (21)$$

where $\mathbb{T}_h^\Gamma = \{T \in \mathbb{T}_h \mid \text{meas}_2(T \cap \Gamma) > 0\}$. Thus $q_j^X \equiv 0$ in all T with $T \notin \mathbb{T}_h^\Gamma$.

In the following we will use the notation $q_j^\Gamma := q_j \Phi_j^H$ and

$$V_h^\Gamma := \text{span}(\{q_j \mid j \in \mathbf{J}\} \cup \{q_j^\Gamma \mid j \in \mathbf{J}_\Gamma\})$$

to emphasize that the extended finite element space V_h^Γ depends on the location of the interface Γ . In particular the dimension of V_h^Γ may change if the interface is moved. The shape of the extended basis functions for the 1D case is sketched in Figure 1.

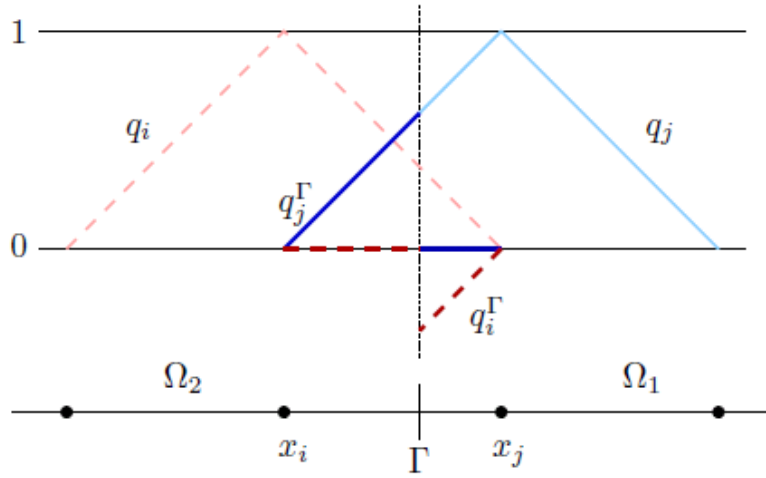


Figure 1: Extended finite element basis functions q_i, q_i^Γ (dashed) and q_j, q_j^Γ (solid) for 1D case.

Note that V_h^Γ can also be characterized by the following property: $q \in V_h^\Gamma$ if and only if there exist functions $q_1, q_2 \in V_h$ such that $q|_{\Omega_i} = q_i|_{\Omega_i}$, $i=1,2$.

For the space V_h^Γ optimal approximation error bounds, both in the L^2 - and H^1 -norm, can be derived. For example, for $p \in L^2(\Omega)$ with $p|_{\Omega_i} \in H^1(\Omega_i)$, $i=1,2$, we have

$$\inf_{q_h \in V_h^\Gamma} \|q_h - p\|_{L^2} \leq ch \|p\|_{1, \Omega_1 \cup \Omega_2}. \quad (22)$$

In [14, 9] this finite element method is used in the numerical simulation of two-phase flow problems.

NUMERICAL EXPERIMENT

We present results of a numerical experiment. These results are from [16] and have been validated by a comparison with measurement data on rise velocities, cf. below. In the

simulation we used the DROPS package [11], in which the finite element methods described above are implemented.

We consider a single n-butanol droplet inside a rectangular tank $\Omega = [0, 12 \cdot 10^{-3}] \times [0, 30 \cdot 10^{-3}] \times [0, 12 \cdot 10^{-3}] m^3$ filled with water, cf. Figure 2. The material properties of this two-phase system are given in Table 1. Initially at rest ($\mathbf{u}_0 = 0 m/s$) the droplet starts to rise in y -direction due to buoyancy effects, with $y = x_2$ and $x = (x_1, x_2, x_3)$.

quantity (unit)	n-butanol	water
ρ (kg/m^3)	845.4	986.5
μ (kg/ms)	$3.281 \cdot 10^{-3}$	$1.388 \cdot 10^{-3}$
τ (N/m)	$1.63 \cdot 10^{-3}$	

Table 1: Material properties of the system n-butanol / water.

For the initial triangulation T_0 the domain Ω is subdivided into $4 \times 10 \times 4$ sub-cubes each consisting of 6 tetrahedra. Then the grid is refined four times in the vicinity of the interface Γ . As time evolves the grid is adapted to the moving interface. Figure 3 shows the droplet and a part of the adaptive mesh for two different time steps. A movie of this numerical simulation is given on the website [11].

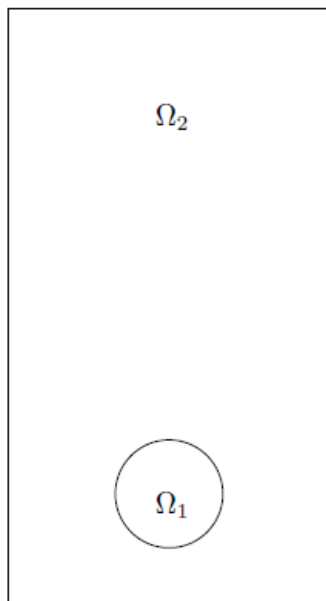


Figure 2: 2D sketch of the rising droplet example.

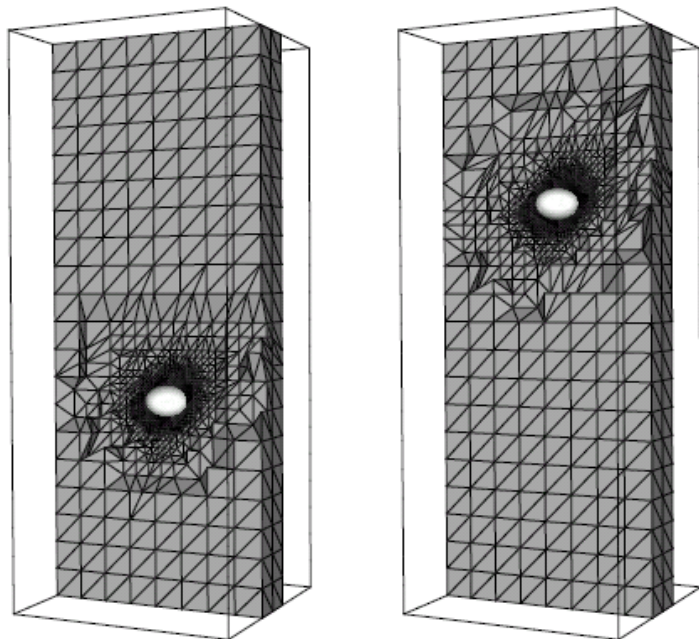


Figure 3: Interface and part of the grid for a rising droplet with radius $r_d = 1mm$ at times $t = 0.2s$ (left) and $t = 0.4s$ (right).

For a butanol droplet with radius $1mm$, in Figure 4 the y -coordinate of the droplet's barycenter \bar{x}_d is shown as a function of time, where

$$\bar{x}_d(t) = \text{meas}_3(\Omega_1(t))^{-1} \int_{\Omega_1(t)} x dx.$$

The average velocity $\bar{\mathbf{u}}_d(t)$ of the drop is given by

$$\bar{\mathbf{u}}_d(t) = \text{meas}_3(\Omega_1(t))^{-1} \int_{\Omega_1(t)} \mathbf{u}(x,t) dx.$$

Note that $\bar{x}_d(t) = \bar{\mathbf{u}}_d(t)$ and, due to incompressibility and immiscibility, $\text{meas}_3(\Omega_1(t)) = \text{meas}_3(\Omega_1(0))$. For a butanol droplet with radius $1mm$ Figure 5 shows the rise velocity, which is the second coordinate of the average velocity $\bar{\mathbf{u}}_d(t)$. After a certain time the rise velocity becomes almost constant and the droplet reaches a terminal rise velocity denoted by u_r . For the radius $r_d = 1mm$ we obtain $u_r = 53mm/s$.

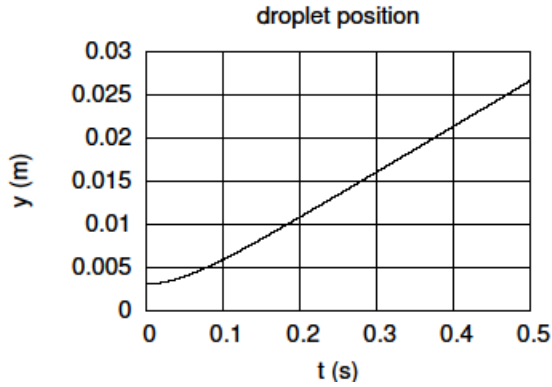


Figure 4: y -coordinate of barycenter of a rising butanol droplet with radius 1 mm as a function of time t .

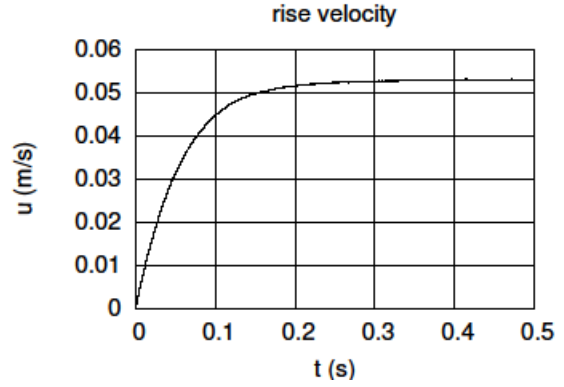


Figure 5: Rise velocity of a butanol droplet with radius 1 mm as a function of time t .

We computed the terminal rise velocities u_r of rising butanol droplets for different drop radii r_d . For larger droplets with $r_d \geq 1.5mm$ a coarser mesh was used (3 times local refinement instead of 4 times as for the smaller droplets) because of memory limitations. A validation of the simulation results by means of comparison with experimental data is given in [5]. In Figure 6, which is taken from [5], the terminal rise velocity u_r is plotted versus the droplet radius r_d and a comparison of experimental and simulation results is shown. For a discussion of these results we refer to [5].

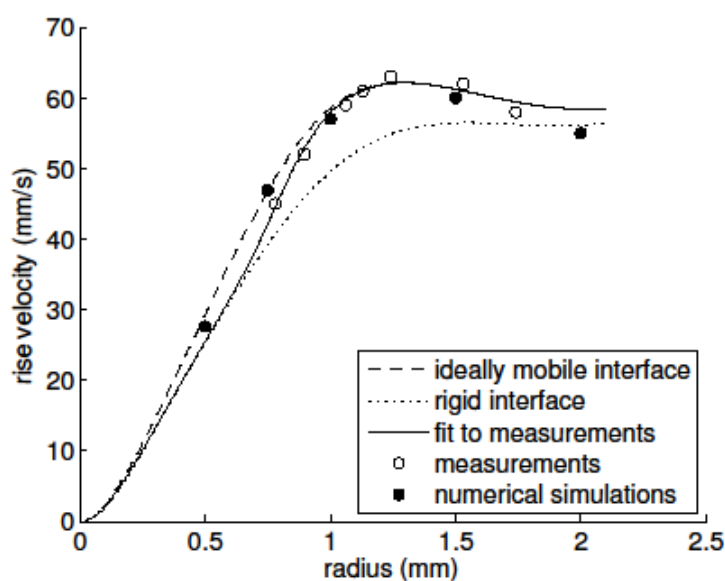


Figure 6: Terminal rise velocities u_r for different droplet radii r_d . Experimental data (open circles), DROPS simulation results (filled circles) and curve fitted to experimental data (solid line).

References

- [1] Aris, R.: Vectors, tensors, and the basic equations of fluid mechanics. Dover Publications, 1989.
- [2] Arnold, D.N. and Brezzi, F. and Cockburn, B. and Marini, L.D.: Unified analysis of discontinuous Galerkin methods for elliptic problems. SIAM J. Numer. Anal., 39 (2002), 1749--1779.
- [3] Bänsch, E.: Finite element discretization of the Navier-Stokes equations with a free capillary surface. Numer. Math., 88 (2001), 203--235.
- [4] Belytschko, T. and Moës, N. and Usui, S. and Parimi, C.: Arbitrary discontinuities in finite elements. Int. J. Num. Meth. Eng., 50 (2001), 993--1013.
- [5] Bertakis, E. and Groß, S. and Grande, J. and Fortmeier, O. and Reusken, A. and Pfennig, A.: Validated simulation of droplet sedimentation with finite-element and level-set methods. Chemical Eng. Science, 65 (2010), 2037--2051.
- [6] Bothe, D. and Prüss, J.: On the two-phase Navier-Stokes equations with Boussinesq-Scriven surface fluid. J. Math. Fluid Mech., 12 (2010), 133--150.
- [7] Burmann, E.: Consistent SUPG method for transient transport problems: stability and convergence. Comput. Methods Appl. Mech. Engrg., 199 (2010), 1114--1123.
- [8] Dziuk, G.: An algorithm for evolutionary surfaces. Numer. Math., 58 (1991), 603--611.

- [9] Esser, P. and Grande, J. and Reusken, A.: An extended finite element method applied to levitated droplet problems. *Int. J. for Numer. Meth. in Eng.*, 84 (2010), 757—773.
- [10] Moës, N. and Dolbow, J. and Belytschko, T.: A Finite Element Method for crack growth without remeshing. *Int. J. Num. Meth. Eng.* 46 (1999), 131—150.
- [11] DROPS package for simulation of two-phase flows.
<http://www.igpm.rwth-aachen.de/DROPS/>.
- [12] Ganesan, S. and Tobiska, L. Finite element simulation of a droplet impinging a horizontal surface. *Proceedings of ALGORITMY 2005*, pages 1--11.
- [13] Groß, S. and Reichelt, V. and Reusken, A.: A Finite Element Based Level Set Method for Two-Phase Incompressible Flows. *Comp. Visual. Sci.* 9 (4) (2006), 239--257.
- [14] Groß, S. and Reusken, A.: An extended pressure finite element space for two-phase incompressible flows with surface tension. *J. Comput. Phys.* 224 (2007), 40--58.
- [15] Groß, S. and Reusken, A.: Finite element discretization error analysis of a surface tension force in two-phase incompressible flows. *SIAM J. Numer. Anal.* 45 (4) (2007), 1679-1700.
- [16] Groß, S. and Reusken, A.: *Numerical Methods for Two-phase Incompressible Flows*. Berlin, Springer, 2011.
- [17] Hesthaven, J.S. and Warburton, T.: *Nodal Discontinuous Galerkin Methods: Algorithms, Analysis, and Applications*. New York, Springer, 2008.
- [18] Hysing, S.: A new implicit surface tension implementation for interfacial flows. *Int. J. Num. Meth. Fluids.* 51 (6) (2006), 659--672.
- [19] Johnson, C. and Nävert, U. and Pitkäranta, J.: Finite element methods for linear hyperbolic problems. *Comput. Methods Appl. Mech. Engrg.*, 45 (1984), 285--312.
- [20] Lishchuk, S. and Halliday, I.: Effective surface viscosities of a particle-laden fluid interface. *Physical Review E*, 80 (2009), 016306.
- [21] Lopez, J. and Chen, J.: Coupling between a viscoelastic gas/liquid interface and a swirling vortex flow. *J. Fluid Eng.* 120 (1998), 655--661.
- [22] Mineev, P.D. and Chen, T. and Nandakumar, K.: A finite element technique for multifluid incompressible flow using Eulerian grids. *J. Comput. Phys.*, 187(1) (2003), 255--273.
- [23] Osher, S. and Fedkiw, R.: *Level Set Methods and Dynamic Implicit Surfaces of Applied Mathematical Sciences*, Vol. 153. Berlin, Heidelberg, New York, Springer, 2003.

- [24] Pillapakam, S. B. and Singh, P.: A level-set method for computing solutions to viscoelastic two-phase flow. *J. Comput. Phys.* 174 (2001), 552--578.
- [25] Reusken, A. and Loch, E.: On the accuracy of the level set SUPG method for approximating interfaces. IGPM report RWTH Aachen, 319 (2011).
- [26] Scriven, L. E.: Dynamics of a fluid interface. Equations of motion for Newtonian surface fluids. *Chem. Eng. Sci.*, 12 (1960) 98--108.
- [27] Sethian, J. A.: *Level Set Methods and Fast Marching Methods*. Cambridge University Press, 1999.
- [28] Sethian, J. A.: Theory, algorithms, and applications of level set methods for propagating interfaces. *Acta Numerica*, 5 (1996), 309--395.
- [29] Slattery, John C. and Sagis, Leonard and Oh, Eun-Seok.: *Interfacial Transport Phenomena*. New York, Springer, Second edition, 2007.
- [30] Sussman, M. and Almgren, A. S. and Bell, J. B. and Colella, Ph. and Howell, L. H. and Welcome, M. L.: An adaptive level set approach for incompressible two-phase flows. *J. Comput. Phys.*, 148 (1999) 81--124.
- [31] Sussman, M. and Smereka, P. and Osher, S.: A level set approach for computing solutions to incompressible two-phase flow. *J. Comput. Phys.*, 114 (1994) 146--159.